Supplementary Information (SI)

For

Simple and rapid gas sensing using a single-walled carbon nanotube field effect transistor-based logic inverter

Salomé Forel [a,1,‡], Leandro Sacco* [a,2,‡], Alice Castan [a,3] Ileana Florea [a], Costel-Sorin Cojocaru [a]*

1. SWCNT-FETs

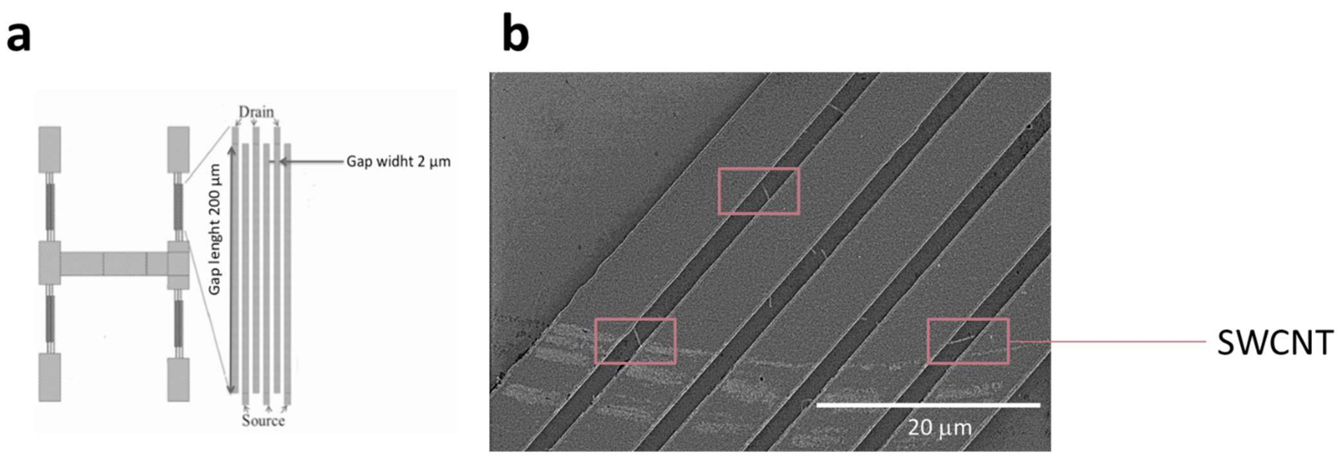

Fig. S1. **a** Schematic view of the transistor geometry **b** Typical scanning electron imaging showing SWCNTs connecting the source and drain electrodes

[a.] *Laboratoire de Physique des Interfaces et des Couches Minces (LPICM), CNRS, Ecole Polytechnique, IP Paris, 91128, Palaiseau Cedex, France.*
Present address
[1.] *Antwerp University, physics department, Experimental Condensed Matter Physics Laboratory, Universiteitsplein 1, 2610 Antwerp, Belgium Email : salome.forel@uantwerpen.be*
[2.] *Delft University of Technology, Faculty of Electrical Engineering, Mathematics and Computer Science, Department of Microelectronics, Delft, Feldmannweg 17, 2628 CT Delft, Netherlands Email : L.N.Sacco@tudelft.nl*
[3.] *Department of Physics and Astronomy, University of Pennsylvania, Philadelphia PA 19104, USA*
† These authors contributed equally.

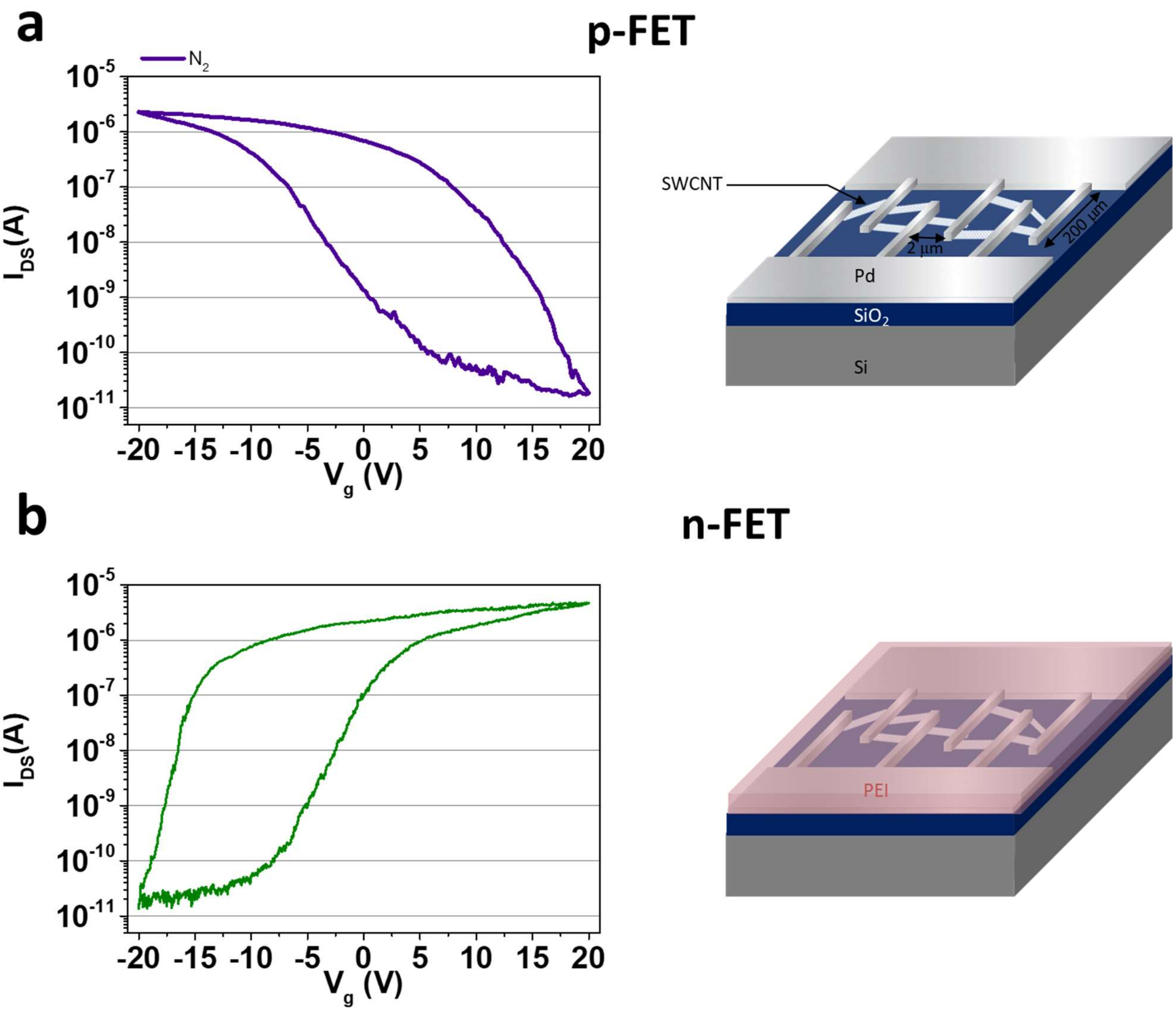

Fig. S2. **a** (left) I_{ds}-V_g characteristic of the p-type SWCNT-FET (V_{DS} = 1 V) (right) schematic view of the p-type SWCNT-FET **b** (left) I_{ds}-V_g characteristic of the n-type SWCNT-FET (V_{DS} = -1 V) (right) schematic view of the n-type SWCNT-FET

2. Gas enclosure characteristic

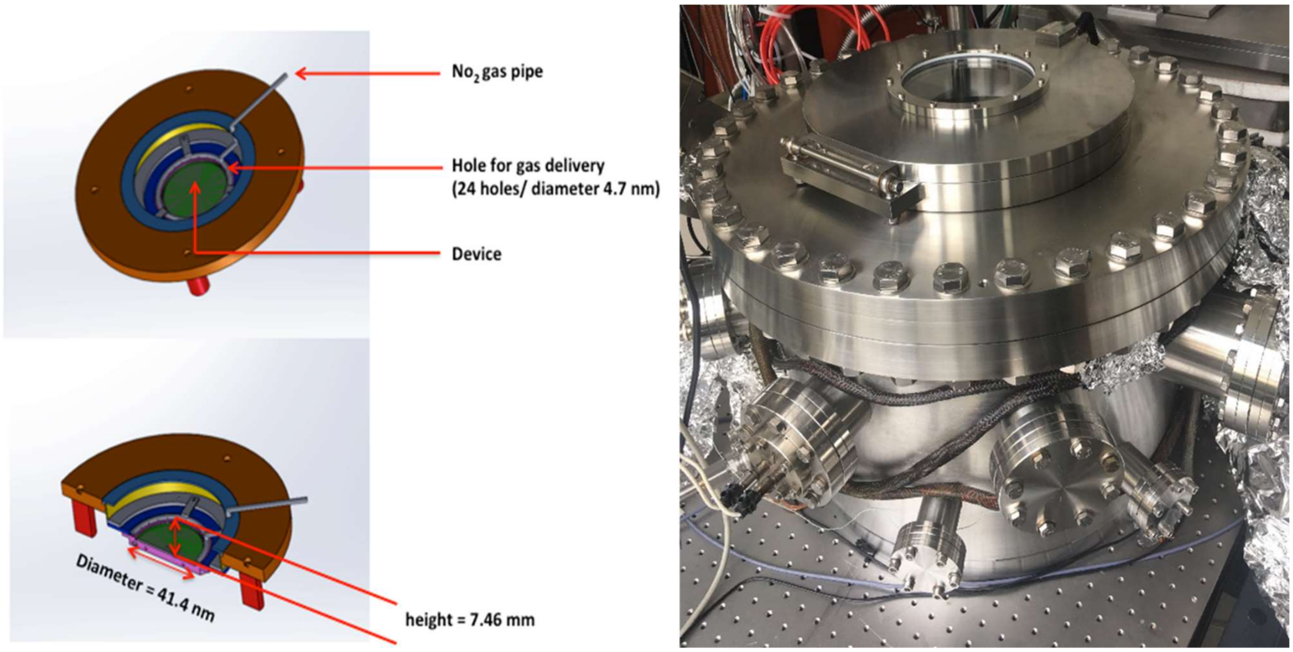

Fig. S3. (left) Schematic view of the gas delivery system (right) picture of the gas enclosure

3. Desorption

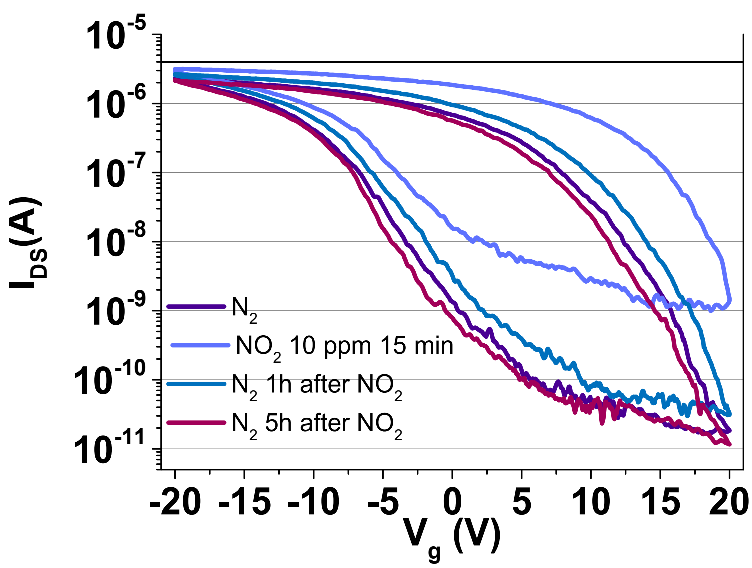

Fig. S4. I_{ds}-V_g curves under N_2 after an exposure to NO_2

4. Device response calculation

The response of the device is taken as shown in the figure. For each defined time (here an example is shown for the response after 15 minutes of gas exposure), the response was considered as the average of half of the V_{out} value on three different pulses (green line sections in Figure S5). The error on V_{out} under N_2 and NO_2 exposures is defined as the standard deviation of the average.

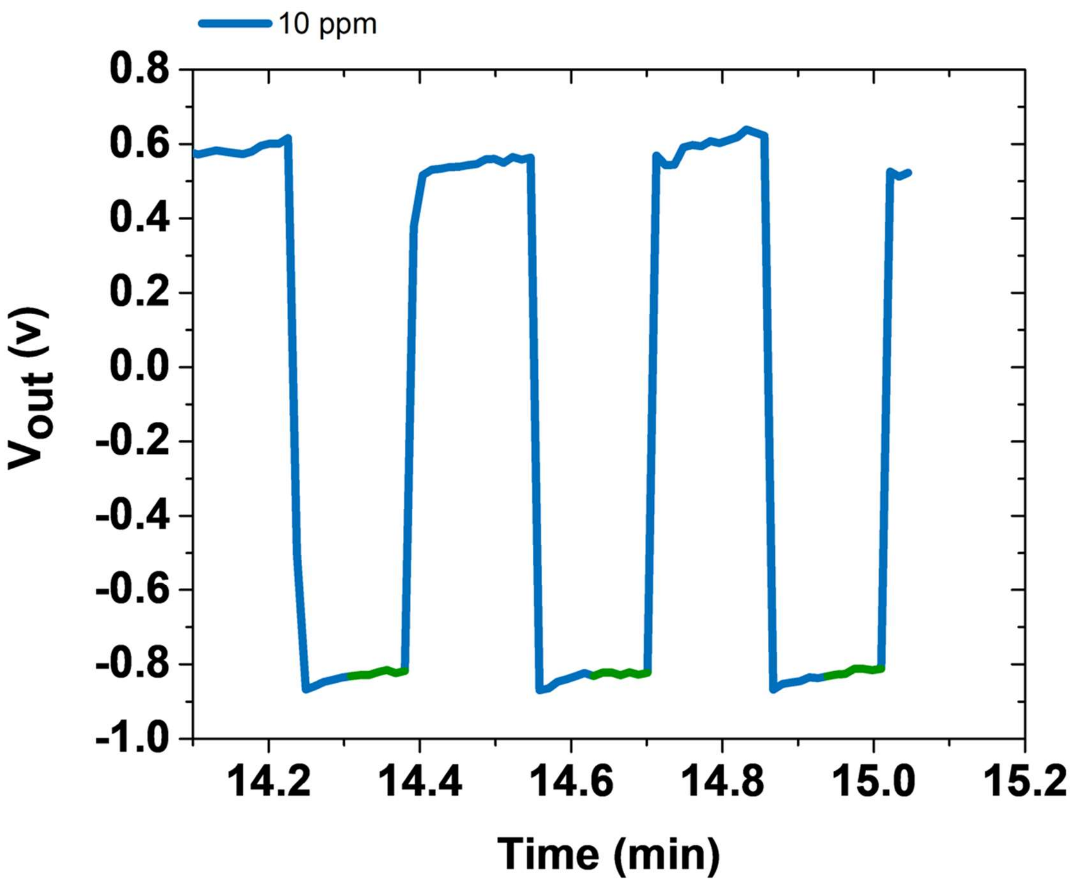

Fig. S5. Output voltage of the inverter after exposure to 10 ppm of NO_2 gas for 15 minutes. The response at 15 minutes is measured using the green sections of the curve.

5. Stability and reproducibility of the response

The reproducibility and stability of the response of our p-device (active part of the sensor) under NO_2 exposure has been tested and reported in a previous work[8], nevertheless the reproducibility of the response of the inverter was also tested. The response of the device was measured for three different NO_2 concentrations (Test 1), and re-measured after several weeks (Test 2).

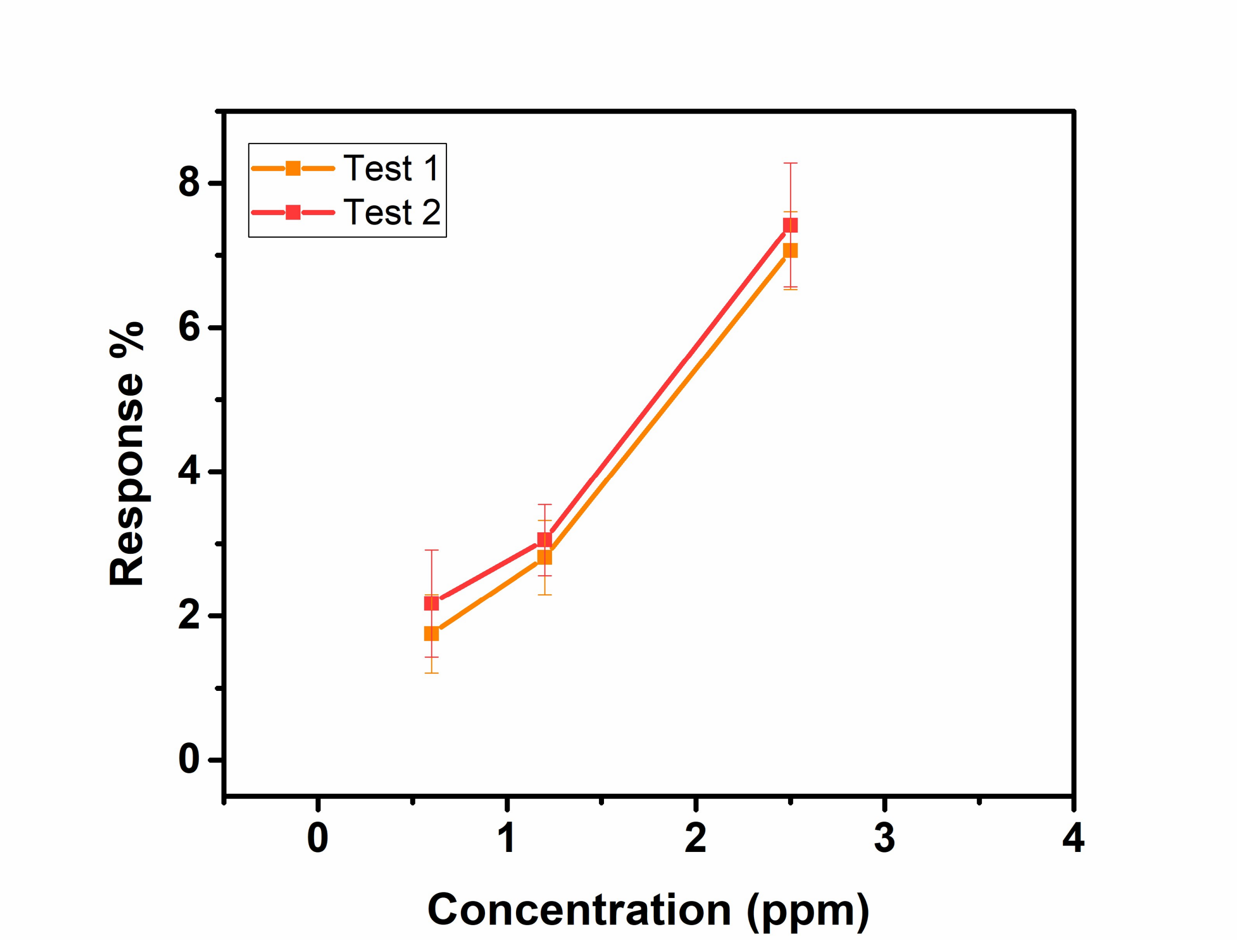

Fig. S6. Response of the same device as a function of NO_2 concentration measured several weeks apart.

6. Output voltage as a function of time under NO_2 exposure

- **V_{DD} = 2 V**

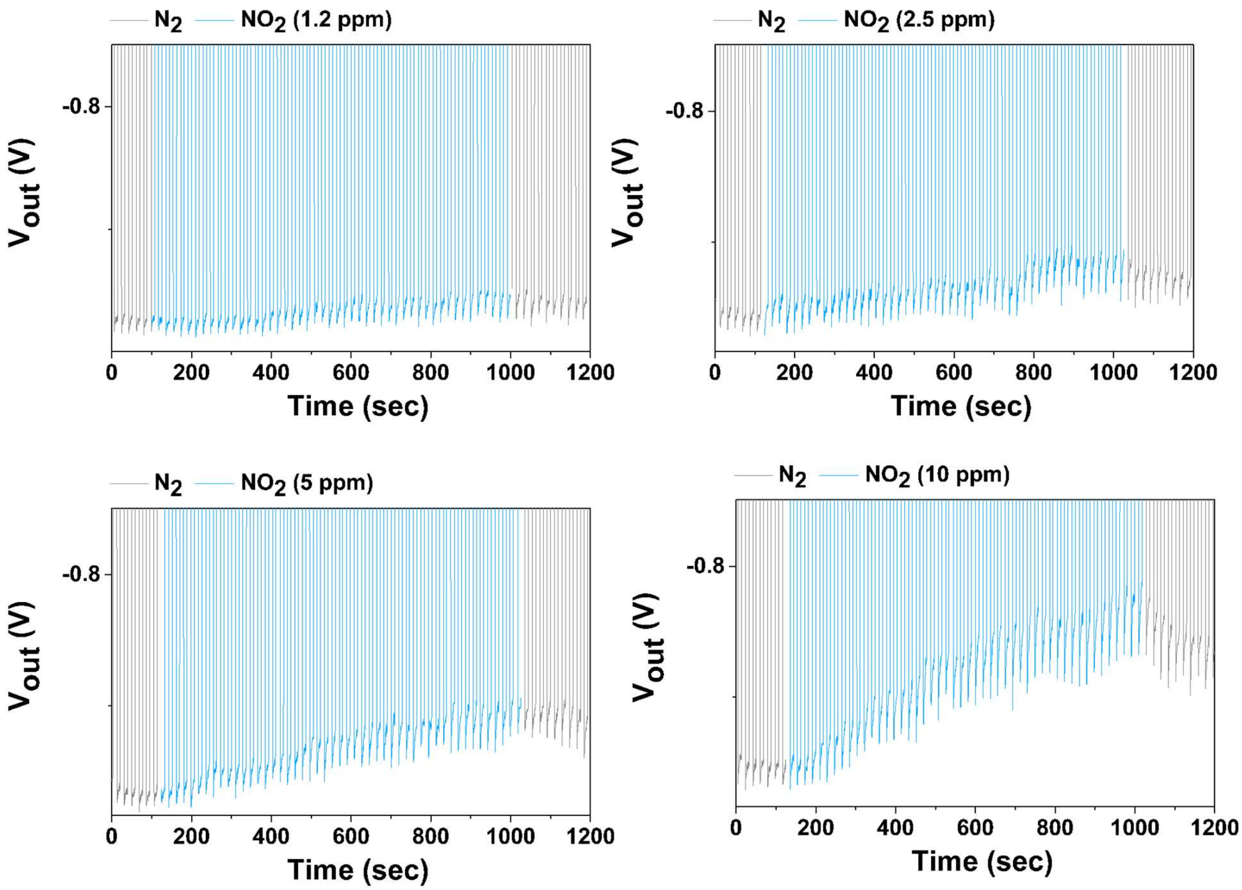

Fig. S7 Output voltage of the inverter as a function of time under NO_2 exposure for a square input voltage of alternatively -4 V and -11 V, **V_{DD} = 2 V.**

- **V_{DD} = 4 V**

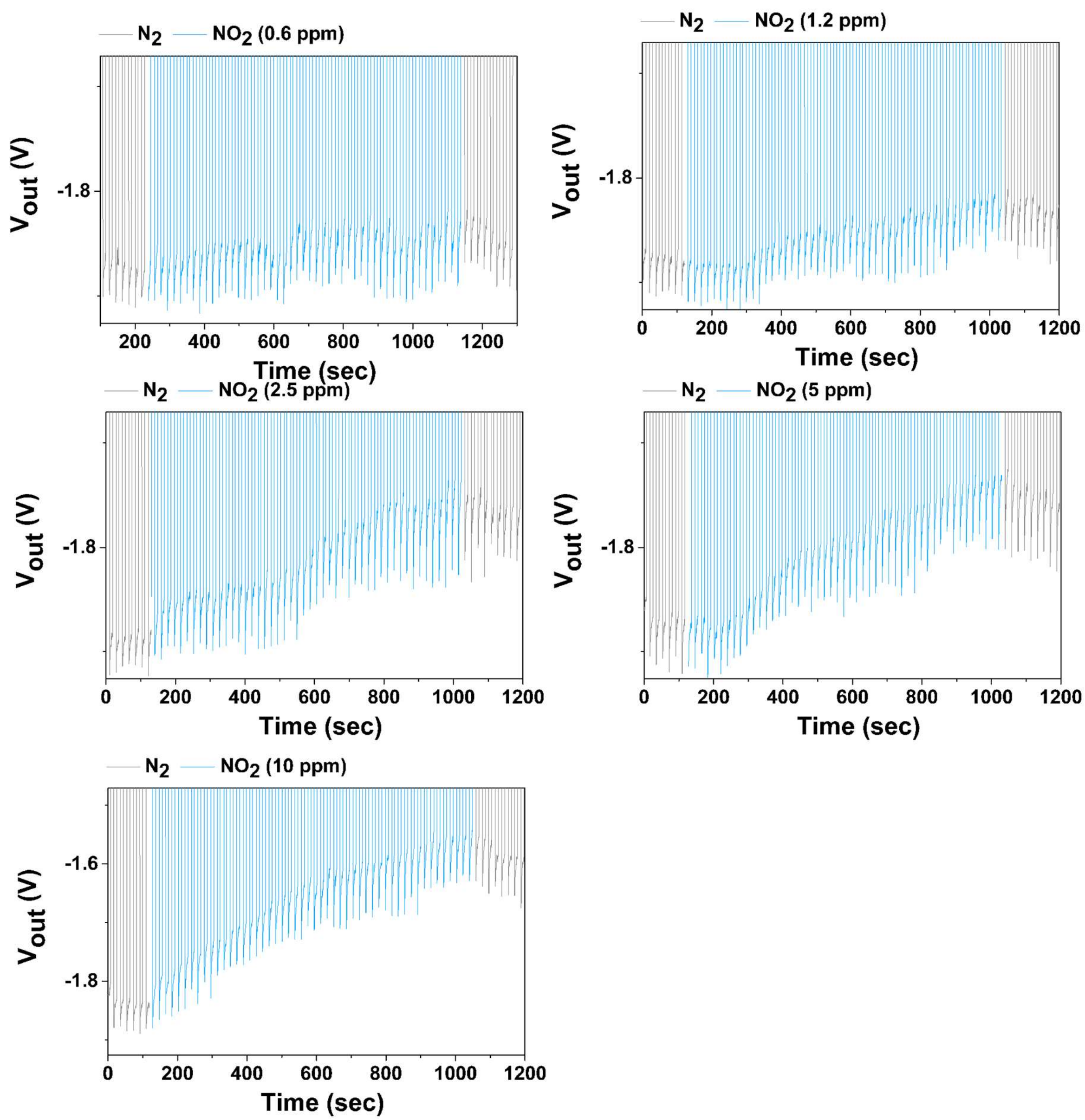

Fig. S8 Output voltage of the inverter as a function of time under NO_2 exposure for a square input voltage of alternatively -4 V and -11 V, **V_{DD} = 4 V.**

- **V_{DD}= 6 V**

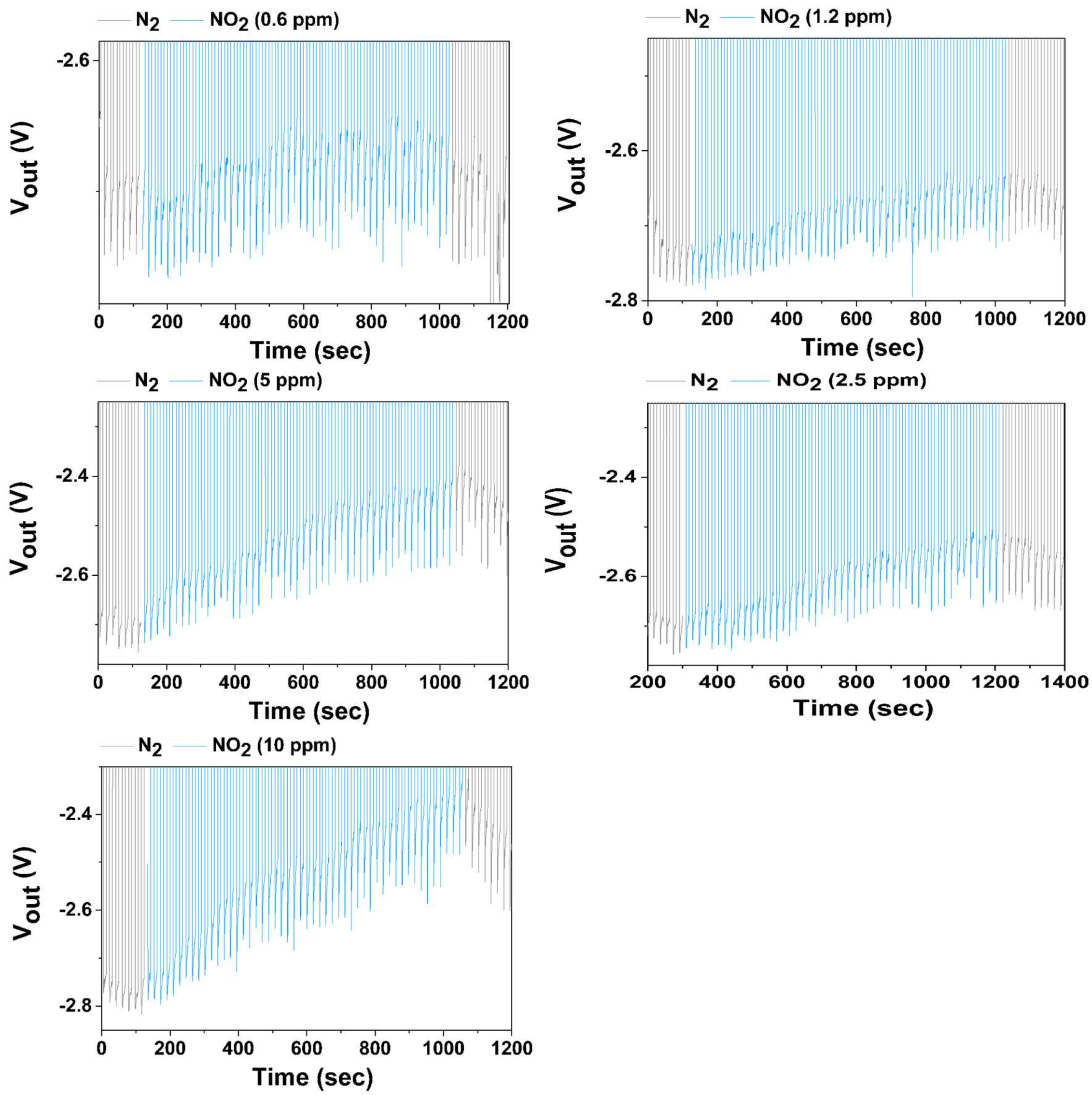

Fig. S9 Output voltage of the inverter as a function of time under NO_2 exposure for a square input voltage of alternatively -4 V and -11 V, **V_{DD} = 6 V.**

7. Limit of Detection (LOD) calculation

For all three V_{DD} used, a calibration curve for low concentrations has been determined by performing a linear fit of the first three points of the curve R=f(C) where R is the response of the device and C the concentration in ppm. The obtained values of r^2 available in Table 1 confirm the linear response of the device in this concentration range.

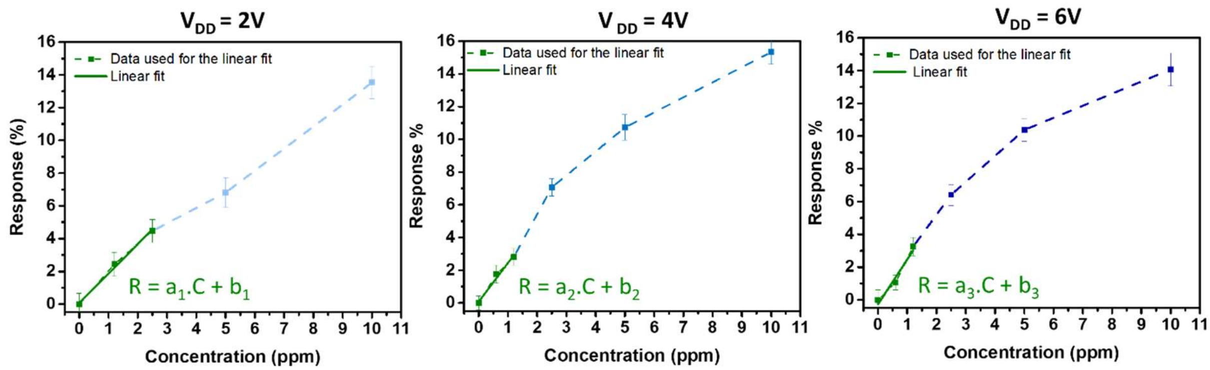

Fig. S10 Response of the device under NO_2 exposure and linear fits at low concentrations (green curve)

V_{DD} (V)	a_i	b_i	r^2
2 (i=1)	1.79127 ± 0.12866	0.08378 ± 0.20042	0.99487
4 (i=2)	2.37032 ± 0.30571	0.08026 ± 0.22286	0.98364
6 (i=3)	2.73325 ± 0.62948	-0.26988± 0.48329	0.94963

Table S1 Parameters of the linear fits.

Then for each V_{DD} used, the response of the device for a concentration C = 0 ppm of NO_2 was measured. The obtained values are detailed in Table 2. According to IUPAC definition the LOD is defined by the lowest discernible signal over the background signal. Here we consider that the lowest response that we can detect as 3 three times the average of the error on the signal of the blank, obtained with at least four measurements of the blank signal. The calculated LOD is given by equation (1):

LOD = 3*blank/slope (1)

V_{DD} = 2 V		V_{DD} = 4 V		V_{DD} = 6 V	
Response C=0	Error	Response C=0	Error	Response C=0	Error
0	0.64632	0	0.43287	0	0.55712
0	0.45518	0	0.45107	0	0.5322
0	0.55686	0	0.5002	0	0.44708
0	0.54666	0	0.36927	0	0.40975
-	-	0	0.5024	0	0.59831
Mean : 0.55+/- 0.08		Mean : 0.45+/-0.05		Mean : 0.51+/-0.08	

Table S2. Response of the device under N_2 (*i.e.* NO_2 concentration at 0 ppm)

The LOD is then obtained using the linear calibration curve, the error is determined using the error on the slope and the standard deviation of the average value of the blank.

V_{DD} (V)	Blank measurement	Blank measurement error	Slope	Slope error	LOD (ppm)	LOD error (ppm)
2	0.55125	0.07814	1.79127	0.12866	0.92	0.20
4	0.45116	0.05494	2.37032	0.30571	0.57	0.14
6	0.50889	0.07829	2.73325	0.62948	0.56	0.21

Table S3. Calculation of the LOD

8. Comparison of SWCNT-FET based devices for NO_2 sensing properties

Device Architecture	Limit of Detection (LOD) [ppm]	Minimum measured Concentration [ppm]	Sensitivity [1/ppm]	Reference
FET sensors based on individual SWCNTs	**-**	**200** **0.3**	**-**	1 2
FET sensors based on individual, suspended SWCNTs	**-**	**1**	**-**	3
FET sensors based on SWCNT networks	**-** **0.044** **0.069**	**20** **6** **0.5**	**-** **0.034 ± 0.002** **0.238**	4 5 6
FET sensors based on low density SWCNT networks	**-**	**0.86**	**-**	7
FET sensors based on few individually connected SWCNTs	**0.086**	**0.1**	**-**	8
Inverter sensors based on p-SWCNT-FET and n-SWCNT-FET containing few individually connected SWCNTs	**0.57 +/- 0.14**	**0.6**	**-**	**This work**

Table S4. Comparison of SWCNT-FET based gas sensor performances.

Reference

1 J. Kong, N. R. Franklin, C. Zhou, M. G. Chapline, S. Peng, K. Cho and H. Dai, *Science*, 2000, **287**, 622–625.

2 M. Lucci, A. Reale, A. Di Carlo, S. Orlanducci, E. Tamburri, M. L. Terranova, I. Davoli, C. Di Natale, A. D'Amico and R. Paolesse, *Sensors Actuators B Chem.*, 2006, **118**, 226–231.

3 K. Chikkadi, M. Muoth, W. Liu, V. Maiwald and C. Hierold, *Sensors Actuators B Chem.*, 2014, **196**, 682–690.

4 M. Jeon, B. Choi, J. Yoon, D. M. Kim, D. H. Kim, I. Park and S.-J. Choi, *Appl. Phys. Lett.*, 2017, **111**, 022102.

5 J. Li, Y. Lu, Q. Ye, M. Cinke, J. Han and M. Meyyappan, *Nano Lett.*, 2003, **3**, 929–933.

6 X. Wang, M. Wei, X. Li, S. Shao, Y. Ren, W. Xu, M. Li, W. Liu, X. Liu and J. Zhao, *ACS Appl. Mater. Interfaces*, 2020, **12**, 51797–51807.

7 K. Xu, C. Wu, X. Tian, J. Liu, M. Li, Y. Zhang and Z. Dong, *Integr. Ferroelectr.*, 2012, **135**, 132–137.

8 L. Sacco, S. Forel, I. Florea and C. Cojocaru, *Carbon N. Y.*, 2020, **157**, 631–639.